Optimal eco-driving for conventional vehicles: Simulation and experiment

Djamaleddine Maamria, Kristan Gillet, Guillaume Colin, Yann Chamaillard, C Nouillant

Optimal eco-driving for conventional vehicles: Simulation and experiment

D. Maamria * **K. Gillet** * **G. Colin** * **Y. Chamaillard** * **C. Nouillant** **

* *Univ. Orléans, PRISME, EA 4229, F45072, Orléans, France.* djamaleddine.maamria@gmail.com, (kristan.gillet, guillaume.colin, yann.chamaillard)@univ-orleans.fr
** *PSA Peugeot Citroën, Direction Recherche Innovation & Technologies Avancées (DRIA), France.* cedric.nouillant@mpsa.com

Abstract: In this paper, the problem of eco-driving for a conventional vehicle equipped with an internal combustion engine is studied. The associated optimal control problem is formulated and solved using Dynamic Programming (DP). The impact of the mesh choice on the optimality of the DP solution is investigated in order to find a trade-off between the optimality of the DP solution and its computation time. The eco-driving speed trajectories obtained were tested on a high-frequency HIL (Hardware-In-the-Loop) engine test bench to quantify the real reductions in fuel consumption. Simulations and experiments are compared.

Keywords: Eco-driving, Dynamic Programming, conventional vehicle, HIL engine test bench

1. INTRODUCTION

Eco-driving is a term used to describe the energy efficient use of vehicles. It is a major way to reduce energy consumption of road transportation system so that less energy is used to travel the same distance (Petit and Sciarretta, 2011; Mensing et al., 2014; Monastyrsky and Golownykh, 1993; Kim et al., 2011a).

In the last decades, engine technology and car performances have improved rapidly, while drivers have not adapted their behavior (driving style). The idea of eco-driving is to determine the velocity trajectory that minimizes the vehicle energy consumption under final time and distance constraints. This question can be formulated as an Optimal Control Problem (OCP) as in (Petit and Sciarretta, 2011; Monastyrsky and Golownykh, 1993; Ozatay et al., 2014; Hellstrom et al., 2010). The eco-driving problem was addressed for conventional vehicles in (F. Mensing, 2013; Sciarretta et al., 2015), for electric cars in (Dib et al., 2014; Petit and Sciarretta, 2011; F. Mensing, 2013; Sciarretta et al., 2015; Miyatake et al., 2011) and for hybrid electric cars in (F. Mensing, 2013; Bouvier et al., 2015; Kim et al., 2011b; Hellstrom et al., 2010; Sciarretta et al., 2015; van Keulen et al., 2010).

In the case of conventional vehicles, fuel consumption, engine emissions or any combination of both over a fixed time window is the cost function to be minimized (Mensing et al., 2011, 2014). Two dynamics are usually considered: the position and the speed of the vehicle while the main constraints bear on speed limitations, vehicle stops and total traveled distance (F. Mensing, 2013; Sciarretta et al., 2015). To solve this kind of OCP, a three dimensional Dynamic Programming (DP) approach was initially used (Mensing et al., 2011; Hooker, 1988). In order to reduce the computational time, a two-dimensional approach was suggested in (Hooker, 1988; Monastyrsky and Golownykh, 1993; F. Mensing, 2013). This two-dimensional approach transforms a time-based OCP into a position-based OCP and introduces a terminal tunable cost to penalize the driving cycle duration (Monastyrsky and Golownykh, 1993; F. Mensing, 2013; Sciarretta et al., 2015).

This paper follows the path described above with the ultimate objective of testing the calculated eco-driving cycles on an HIL (Hardware In The Loop) test bench. Few studies (F. Mensing, 2013) in the literature deal with the experimental validation of eco-driving cycles on a test bench. The main reason is that the model of fuel consumption used for DP is a quasi-static model and many phenomena are neglected. For example, in the model used by DP, the gear-box ratio shifting is assumed to be instantaneous.

The case under consideration in this paper is a conventional vehicle equipped with a Diesel engine. Six normalized driving cycles are considered. In a first step, the eco-driving cycles are calculated using DP. Initial and eco-driving cycles are then tested on the test bench. Comparisons between the simulation and the experiment results in terms of fuel consumption reduction and state trajectories is performed.

The paper is organized as follows. In Section 2, the vehicle model is described. The calculation of eco-driving cycles using DP is presented in Section 3. Section 4 discusses numerical results. The test bench description and the experimental results are detailed in Section 5. Finally, some conclusions and perspectives are given in Section 6.

2. VEHICLE MODELING

2.1 Motion equations

The vehicle is modeled in a vertical plane. According to Newton's law of motion, the vehicle speed v satisfies

$$(m+m_{rot})\cdot\frac{dv(t)}{dt}=F_t(t)-F_r(t), \tag{1}$$

where F_t is the traction force provided by the engine, F_r is the sum of resistance forces and m is the total vehicle mass.

The term m_{rot} is an equivalent mass of the rotating parts. The force F_r comprises the rolling resistance force, the aerodynamic drag force and a force due to the road grade. Its expression is given by

$$F_r(t) = c_0 + c_1 \cdot v(t) + c_2 \cdot v(t)^2, \quad (2)$$

where c_i, $i = \{0,1,2\}$ are the coefficients of the road load equation. This model considers only the forces in the longitudinal direction. All latitudinal forces, variations of friction parameters during curves, wind forces, and other disturbances are neglected.

2.2 Internal Combustion Engine (ICE)

The ICE under consideration (available in the test bench) is a Diesel engine. This choice is not restrictive and the same methodology can be extended to a gasoline engine. The fuel consumption $\dot{m}_f$ (g/s) is computed through a *measured* look-up table (see Figure 1) as a function of the engine torque T_{eng} and engine speed ω_{eng}

$$\dot{m}_f = \dot{m}_f(\omega_{eng}, T_{eng}).$$

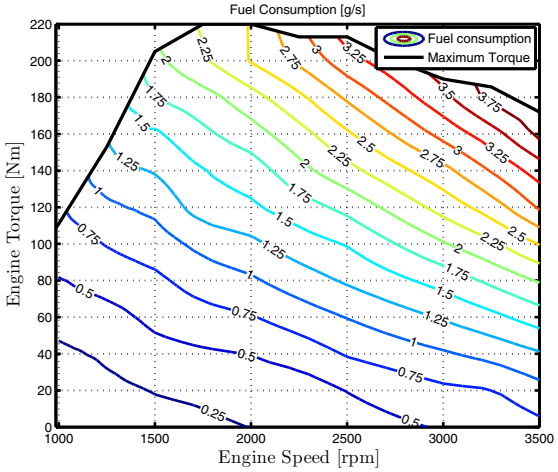

Fig. 1. Measured fuel consumption (g/s) of the ICE.

2.3 Transmission

The engine torque T_{eng} is related to the driver's torque demand at the wheel T_{wh} by

$$T_{wh}(t) = r_{tire} \cdot F_t(t) = \eta_{gb} \cdot R_{gb}(t) \cdot R_t \cdot T_{eng}(t), \quad (3)$$

where R_{gb} is the gear-box ratio, η_{gb} is the gear-box efficiency (assumed to be constant) and R_t is the differential ratio. The torque T_{wh} can be positive (traction) or negative (braking). Similarly, the rotational speed ω_{eng} of the ICE is related to the vehicle speed v by

$$\omega_{eng}(t) = R_{gb}(t) \cdot R_t \cdot \frac{v(t)}{r_{tire}}.$$

The model parameters are summarized in Table 1. The gear-box considered has 5 ratios. The coefficients of the road load are omitted for confidentiality reasons.

3. PROBLEM FORMULATION AND SOLVING METHOD

For a given road, eco-driving consists of finding the best speed profile minimizing the vehicle fuel or power consumption. The vehicle starts from a point A at a velocity v_0 (≥ 0) and must reach a destination point B at time t_f, with a velocity v_1 (≥ 0) (Dib et al., 2014; Mensing et al., 2014). This kind of problem can be solved using optimal control tools (Petit and Sciarretta, 2011; Mensing et al., 2014).

Table 1. Vehicle model parameters

	Description	Value	Unit
m	Vehicle mass	1075	kg
r_{tire}	Wheel radius	0.3014	m
j_{tire}	Wheel inertia	1.07	kg·m^2
η_{gb}	Gear-box efficiency	0.92	–
R_t	Differential ratio	4.06	–
ω_{idle}	Engine idle speed	800	rpm
ω_{min}	Min value of engine speed	1000	rpm
ω_{max}	Max value of engine speed	3500	rpm
a_{min}	Acceleration min value	-2	m/s^2
a_{max}	Acceleration max value	1	m/s^2

3.1 OCP formulation

The cost function to be minimized is the fuel consumption over a fixed time window of duration t_f:

$$J = \int_0^{t_f} \dot{m}_f(\omega_{eng}(t), T_{eng}(t))dt.$$

The control variable U (*to be optimized*) is composed of two components: the engine torque T_{eng} and the gear-box ratio R_{gb}

$$U(t) = [T_{eng}(t),\ R_{gb}(t)].$$

This optimization is carried out under the dynamical constraints

$$\frac{dv(t)}{dt} = f(v(t), U(t)),\ v(0) = v_0, \quad (4)$$

$$\frac{dx(t)}{dt} = v(t), \qquad x(0) = 0, \quad (5)$$

where x is the position of the vehicle and the function f is calculated by combining (1, 2, 3)

$$f = \frac{1}{m + m_{rot}}(-c_0 - c_1 \cdot v - c_2 \cdot v^2 + \frac{\eta_{gb}}{r_{tire}} \cdot R_{gb} \cdot R_t \cdot T_{eng}).$$

Since the speed, the engine torque and the gear-box ratio are limited and the final position and the final speed are fixed, the optimization must be performed under the following constraints

$$v(t) \in [0,\ v_{max}(x(t))], \quad (6)$$

$$f(v(t), U(t)) \in [a_{min},\ a_{max}], \quad (7)$$

$$T_{eng}(t) \in [T_{min}(\omega_{eng}(t)),\ T_{max}(\omega_{eng}(t))], \quad (8)$$

$$\omega_{eng}(t) \in [\omega_{min},\ \omega_{max}], \quad (9)$$

$$x(t_f) = D, \quad (10)$$

$$v(t_f) = v_1, \quad (11)$$

where D is the total traveled distance, T_{min} and T_{max} are given by look-up tables as a function of the engine rotation speed ω_{eng}. In addition, the vehicle acceleration is constrained in (7). The speed limitations are given as a function of the vehicle position and not of time (Mensing et al., 2011; Dib et al., 2014).

To summarize, the OCP considered in this paper is

$$(OCP):\ \min_U \int_0^{t_f} \dot{m}_f(v, U)dt \quad (12)$$

under the dynamics (4, 5), the state and input constraints (6, 7, 8, 9), and the final constraints (10, 11). The considered initial and final values of the vehicle speed in this study are zero

$$v_0 = v_1 = 0.$$

3.2 Solving method

The proposed method is based on dynamic programming (Bertsekas, 2012; Bryson and Ho, 1969). The chosen approach transforms a time-based OCP into a distance-based OCP as suggested in (F. Mensing, 2013; Monastyrsky and Golownykh, 1993; Bouvier et al., 2015) in order to reduce the computation time (a comparison between the time-based and the space-based OCP solutions is given in (Maamria et al., 2016)).

In the space-based OCP, the stop phases are removed from the driving cycle. If the position space is discretized in N steps, the time step $\Delta t(k),\ k = 1:N$ is variable and is calculated from the vehicle speed $v(k)$ and the vehicle acceleration $a(k)$ by solving the following second order equation (F. Mensing, 2013)

$$\Delta x = \frac{1}{2} a(k) \cdot \Delta t(k)^2 + v(k) \cdot \Delta t(k),$$

where Δx is the *fixed* distance step. The acceleration $a(k)$ is calculated from the vehicle speed $v(k)$ and the control variables $U(k)$. The final constraint on the vehicle position (10) is fulfilled by construction. In order to reduce the calculation time, an additional tunable term $\beta \cdot \Delta t(k)$ is added to the cost function as follows

$$\bar{J}_s(u) = \sum_{k=1}^{k=N} \left[\dot{m}_f(v(k), U(k)) + \beta \right] \Delta t(k).$$

The constant tunable parameter β penalizes the final time to obtain almost the same time duration as the initial driving cycle: the study in (F. Mensing, 2013; Maamria et al., 2016) shows that the relation between $t_f = \sum_{k=1}^{N} \Delta t(k)$ and β is monotone. A root-finding method could be used to drive the final time error to zero (Mensing et al., 2011; Sciarretta et al., 2015).

3.3 Speed trajectory computation

To compute an eco-driving cycle, the following constraints (Mensing et al., 2014) have to be included:

- the same final distance $x(t_f)$, the same number of stops and the same duration t_f as the initial driving cycle,
- the vehicle speed limitations depending on the position of the vehicle (x).

In this study, to specify the speed limits, a certain (fixed) margin e_l on the initial driving cycle speed is considered, for each time t

$$v_{max}(x(t)) = \begin{cases} v(x(t)) + e_l, & v(x(t)) > 0, \\ 0, & v(x(t)) = 0, \end{cases}$$

where $v(x(t))$ is the speed value of the initial cycle at the position $x(t)$. The value of e_l considered here is 4km/h. When the value of e_l decreases, the fuel saving decreases, and vice versa. Other type of limits can be considered (see (F. Mensing, 2013; Bouvier et al., 2015)) and the choice of speed limits does not impact the solving method (the choice will change the optimal speed trajectories). Then, the objective is to find a new speed trajectory that takes these constraints into account and leads to a lower fuel consumption where the vehicle stops are relevant in distance and not in time (F. Mensing, 2013).

4. NUMERICAL RESULTS

Six normalized driving cycles are selected: EUDC (the Extra-urban driving cycle), NEDC (the New European driving cycle), WLTC (the Worldwide harmonized Light vehicles Test Cycle), the Middle phase of the WLTC, the Artemis Urban and Artemis Rural driving cycle. The *duration without stop phases*, the total traveled distance and the mean value of the vehicle speed are given in Table 2. *We recall that the stop phases are removed from the driving cycles.*

The value of β is calculated in order to have almost the same duration as the initial driving cycle (with an error less than 0.3% on the final time t_f).

Table 2. Driving cycle parameters

Cycle Name	Duration [s]	Distance [km]	Mean speed $\bar{v}$ [km/h]
EUDC	360	6.9	69
A. Rural	1053	17.26	59
WLTC	1574	22.72	52
Middle-WLTC	386	5	46.6
NEDC	900	10.95	43.8
A. Urban	682	4.45	23.5

In this section, the impact of the mesh choice on the optimality of the solution and the state trajectories is investigated. The objective is to show that it is possible to find a trade-off between the optimality of the solution and the time needed to run the DP. A standard laptop equipped with an Intel Core i7-2820 QM 2.30GHz with 8GB of RAM is used. The numerical analysis is limited to two driving cycles: NEDC and WLTC.

Several meshes for the speed (v) and the engine torque (u) are tested: the distance step is $dx = 10$m and a spacing of 1 (from 1 to 5) for the gear-box ratio R_{gb} is chosen. The obtained speed trajectories for the NEDC cycle are shown in Figure 2 versus distance and in Figure 3 versus time (respectively in Figures 4 and 5 for the WLTC cycle).

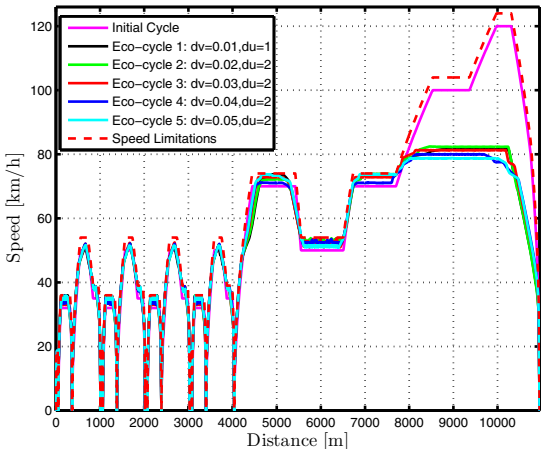

Fig. 2. Vehicle speed [km/h] vs distance [m] for NEDC cycle.

Figures 2, 3, 4 and 5 show that the speed trajectories are slightly impacted by the mesh choice. In the NEDC case, for the meshes [$dv = 0.02$m/s, $du = 2$N.m] and [$dv = 0.03$m/s, $du = 2$N.m], the speed trajectories are relatively close to the trajectory calculated for [$dv = 0.01$m/s, $du = 1$N.m] (considered as a reference in this study). The Eco-cycles calculated for [$dv = 0.04$m/s, $du = 2$N.m] and [$dv = 0.05$m/s, $du = 2$N.m] are quite different

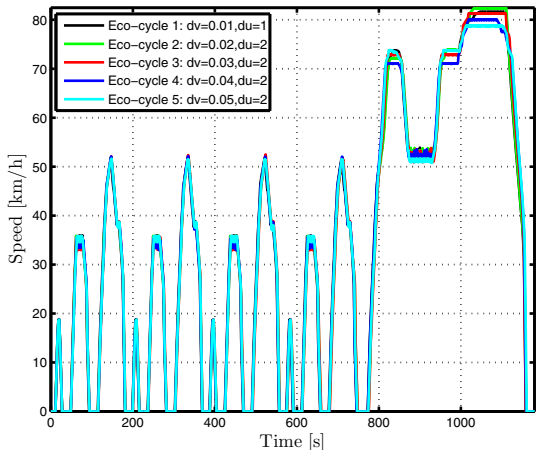

Fig. 3. Vehicle speed [km/h] vs Time [s] for NEDC cycle.

from the reference cycle [$dv = 0.01$m/s, $du = 1$N.m], mainly at high vehicle speed. This remark holds also for the WLTC cycle.

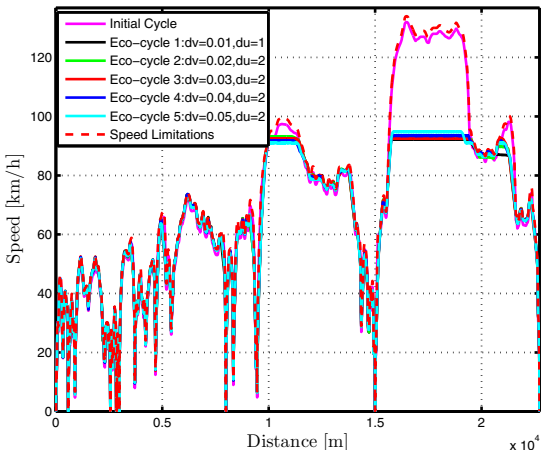

Fig. 4. Vehicle speed [km/h] vs distance [m] for WLTC cycle.

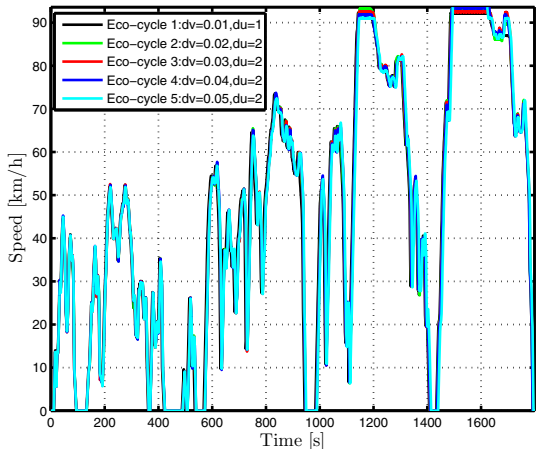

Fig. 5. Vehicle speed [km/h] vs Time [s] for WLTC cycle.

In order to analyze the impact of the mesh choice on the optimality, the fuel consumption [L/100km] and the computation time α needed to run the DP for each iteration are given in Table 3 for the NEDC (respectively in Table 4 for the WLTC) where: dv represents the speed step in [m/s] and du represents the engine torque step in [N.m].

Table 3. Computation time α [s], fuel consumption [L/100km] and the final time t_f [s]: NEDC cycle.

	dv	du	Consumption	α	t_f
Initial cycle	–	–	3.76	–	900
Eco-cycle 1	0.01	1	2.60	1039	899.4
Eco-cycle 2	0.02	2	2.61	267	899.4
Eco-cycle 3	0.03	2	2.63	195	899.25
Eco-cycle 4	0.04	2	2.638	133	899.3
Eco-cycle 5	0.05	2	2.644	104	900.2

For Eco-cycle 3, the fuel consumption is very close to the fuel consumption for Eco-cycle 1 (with an induced sub-optimality less than 1.5%) while the computation time is divided by 5.3 for the NEDC and by 5.7 for the WLTC. For Eco-cycle 4, the induced sub-optimality compared to Eco-cycle 1 is 1.5% for the NEDC (respectively 2.2% for the WLTC) while the time needed to run the DP is divided by 7.8 (respectively by 7.7 for the WLTC). Thus, the DP solution for the mesh [$dv = 0.04$m/s, $du = 2$N.m] can be considered as accurate enough to guarantee a quasi-optimal fuel consumption while requiring an acceptable computation time. A similar analysis was conducted for the other driving cycles (EUDC, the Middle phase of the WLTC, the Urban Artemis and Artemis Rural cycles) and the conclusion is that the mesh [$dv = 0.04$m/s, $du = 2$N.m] is a good trade-off between the optimality of the DP and its computation time.

Table 4. Computation time α [s], fuel consumption [L/100km] and the final time t_f [s]: WLTC cycle.

	dv	du	Consumption	α	t_f
Initial cycle	–	–	3.93	–	1574
Eco-cycle 1	0.01	1	3.06	2340	1570.8
Eco-cycle 2	0.02	2	3.10	605	1571.4
Eco-cycle 3	0.03	2	3.11	405	1572.4
Eco-cycle 4	0.04	2	3.13	303	1571.0
Eco-cycle 5	0.05	2	3.149	241	1573.0

Furthermore, eco-driving cycles do not reach the high speed area (see Figure 2 after 8km and Figure 4 after 15km). The DP chooses to go faster than the initial driving cycle at low vehicle speeds and to go slower at high vehicle speeds. This is possible because of the degree of freedom on the speed limitations (e_l). When e_l decreases, the speed of the eco-driving cycle comes closer to the initial driving cycle speed and fuel saving decreases.

5. EXPERIMENTAL RESULTS

5.1 Test bench description

The HyHIL test bench is composed of an engine connected to a high-dynamics generator with a transmission (see Figure 6). A vehicle model is implemented in the test bench supervision software and simulated in real-time. A driver model controls the vehicle speed to track the vehicle speed set-points given from the driving cycle (the driver model is a PID controller). The requested torque is deduced from the driver demand. The engine torque is measured with a torque-meter on the crankshaft and used by the vehicle model to compute the vehicle speed. The instantaneous fuel consumption is measured using a *Coriolis*

flow meter (manufacturer: Brooks Instrument). Similar HyHIL experiments have been described in (Perez et al., 2008; Chasse et al., 2010; Michel et al., 2015).

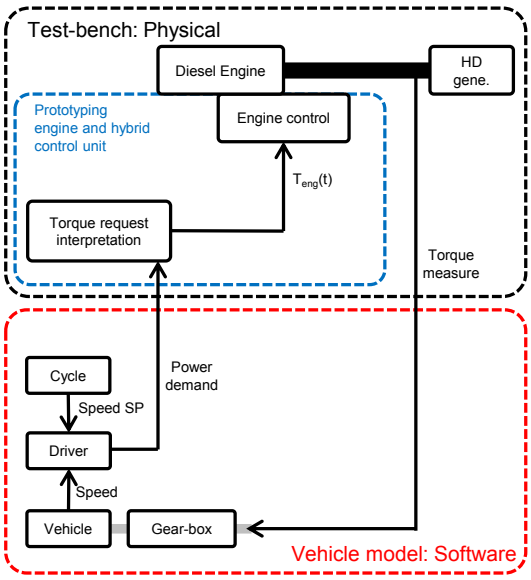

Fig. 6. Schematic of the Hy-HIL test bench

5.2 Procedure and Results

As mentioned above, the OCP in (12) is solved with a fixed distance step. The obtained time step is variable depending on the vehicle speed (the time step is implicitly calculated based on the vehicle speed, vehicle acceleration and traveled distance). To be able to test the eco-driving cycles on a test bench, a fixed time step of 1s is required. the proceed is the following:

(1) An eco-driving cycle is calculated using DP.
(2) The speed and the gear-box ratios are interpolated (linearly) on a new time vector with a fixed step of 1s.

The 6 initial driving cycles and their corresponding eco-driving cycles are tested. The vehicle speed, the accumulated fuel consumption, the gear-box ratio and the torque needed to follow the driving cycles for the EUDC case are given in Figures 7, 9, 8 and 10, respectively. This cycle is the most appropriate to be analyzed as it is short and does not have stops. For the other driving cycles, a zoom on the trajectories is necessary.

Figure 7 shows that the vehicle speed in the simulation and in the experiments are very close. The gear-box ratios for the eco-driving cycle are well managed in the optimization. The only noticeable difference is in the engine torque trajectories (Figure 10) mainly because of the gear-box ratio shifting: in the simulation, the gear-box ratio shifting is assumed to be instantaneous, but it takes 0.5s in the test bench to change the gear-box ratio (see the torque drop in Figure 10 in the beginning of the driving cycle). Moreover, the eco-drivng cycle goes faster than the initial cycle at low vehicle speed (with a slightly higher fuel consumption as shown in Figure 9 between $t = 0$s and $t = 250$s) and goes slower than the initial cycle at high vehicle speed (with a lower fuel consumption as shown in Figure 9 during the time interval $t \in [250\text{s}, 360\text{s}]$).

To compare the simulations and the experiments from an optimality viewpoint, the reductions in fuel consumption are given

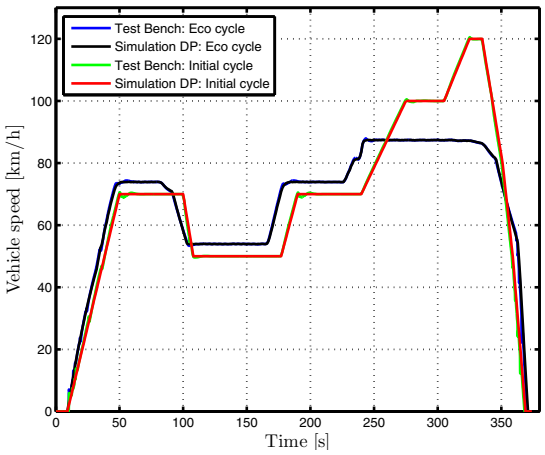

Fig. 7. Vehicle speed trajectory [km/h] for the EUDC.

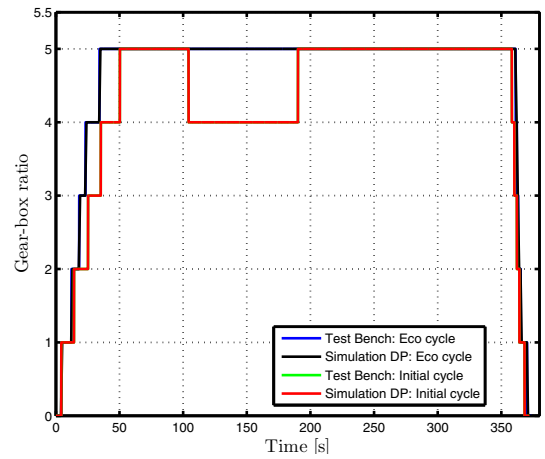

Fig. 8. Gear-box ratio trajectory for the EUDC.

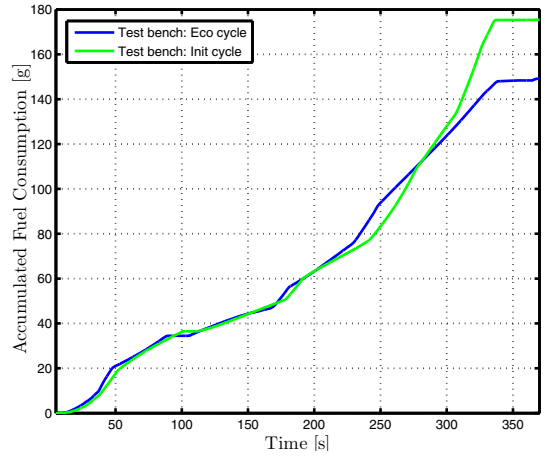

Fig. 9. Accumulated fuel consumption [g] for the EUDC.

in Table 5 (column **Exp**). The experiments on the test bench were repeated three times and the mean value of the fuel consumption for the various tests was taken (the difference in the fuel consumption between several tests was less than 1%). From Table 5, simulations and experiments are very close in terms of fuel reduction: the maximum difference is 3.7% in the case of NEDC and 3.1% in the case of the Artemis Rural. For the other driving cycles, the difference is less than 2%. These

fuel reductions are *implicit upper bounds* on fuel saving that one can obtain through eco-driving.

Furthermore, fuel consumption saving is correlated to the speed mean value of the initial driving cycle ($\bar{v}$) given in Table 2: fuel consumption reduction increases when $\bar{v}$ decreases. For the EUDC cycle, the fuel saving is 16.3% while for the urban Artemis case, the fuel saving is 40%. this can be explained by the fact that when the vehicle speed is low, a great margin for fuel saving improvement is possible.

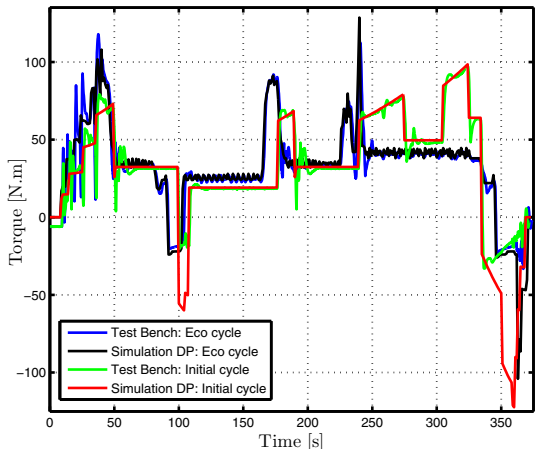

Fig. 10. Torque T_{eng} [N.m] needed to follow the EUDC. The positive part (traction) is provided by the engine while the negative part includes the engine frictions and the braking system.

Table 5. Fuel consumption [g] and fuel saving [%]

	Initial cycle		Eco cycle		Fuel saving [%]	
	Sim	Exp	Sim	Exp	Sim	Exp
EUDC	181.3	175.5	151.8	149.3	16.3	15
A. Rural	461.1	473.4	370.9	396.4	19.4	16.4
WLTC	652.2	650.3	518.1	530.9	20.6	18.5
Middle	114.5	116.1	86.7	88.1	24.3	24.1
NEDC	296.6	276.3	213.87	209.6	27.9	24.2
A. Urban	147.6	165.3	88.7	93.6	39.9	43.3

6. CONCLUSION

The eco-driving problem for conventional vehicles has been addressed and solved using DP. In a first step, the impact of the mesh choice on the solution was studied numerically. Based on the presented results, it is possible to find a good trade-off between the optimality of the solution and the DP computation time. In a second step, the (initial and eco) driving cycles were tested on an HIL test bench. The simulation and the experimental results are *close* in terms of fuel consumption reduction and this reduction depends on the nature of the driving cycle (urban or highway). These gains give *implicit upper bounds* on fuel saving through an eco-driving methodology. It is planned to take pollutant emissions into account in the calculation of eco-driving cycles. This will be the subject of future investigations.

REFERENCES

Bertsekas, D. (2012). *Dynamic programming and optimal control*. Athena Scientific.

Bouvier, H., Colin, G., and Chamaillard, Y. (2015). Determination and comparison of optimal eco-driving cycles for hybrid electric vehicles. *European Control Conference*, 142–147.

Bryson, A.E. and Ho, Y.C. (1969). *Applied optimal control*. Ginn and Company: Waltham, MA.

Chasse, A., Corde, G., Mastro, A.D., and Perez, F. (2010). Online optimal control of a parallel hybrid with after-treatment constraint integration. *IEEE Vehicle Power and Propulsion Conf, Lille (France)*.

Dib, W., Chasse, A., Moulin, P., Sciarretta, A., and Corde, G. (2014). Optimal energy management for an electric vehicle in eco-driving applications. *Control Engineering Practice*, 29, 299–307.

F. Mensing (2013). *Optimal energy utilization in conventional, electric and hybrid vehicles and its application to eco-driving*. Ph.D. thesis, INSA Lyon.

Hellstrom, E., Aslund, J., and Nielsen, L. (2010). Design of an efficient algorithm for fuel-optimal look-ahead control. *Control Engineering Practice*, 18, 13181327.

Hooker, J. (1988). Optimal driving for single-vehicle fuel economy. *Transportation Research-A*, 183–201.

Kim, S.Y., Shin, D.J., and Yoon, H.J.e.a. (2011a). Development of eco-driving guide system. *In SAE asia pacific automotive engineering conference*, 1636–1641.

Kim, T.S., Manzie, C., and Sharma, R. (2011b). Two-stage optimal control of a parallel hybrid vehicle with traffic preview. *IFAC Proceedings Volumes*, 44, 21152120.

Maamria, D., Gillet, K., Colin, G., Chamaillard, Y., and Nouillant, C. (2016). Which methodology is more appropriate to solve eco-driving optimal control problem for conventional vehicles? *IEEE MSC*.

Mensing, F., Bideaux, E., Trigui, R., Ribet, J., and Jeanneret, B. (2014). Eco-driving: an economic or ecologic driving style? *Transportation Research Part C: Emerging Technologies*, 38, 110–121.

Mensing, F., Trigui, R., and Bideaux, E. (2011). Vehicle trajectory optimization for application in eco-driving. *IEEE Vehicle Power and Propulsion Conference*, 1–6.

Michel, P., Charlet, A., Colin, G., Chamaillard, Y., Bloch, G., and Nouillant, C. (2015). Optimizing fuel consumption and pollutant emissions of gasoline-hev with catalytic converter. *Control Engineering Practice*.

Miyatake, M., Kuriyama, M., and Takeda, Y. (2011). Theoretical study on ecodriving technique for an electric vehicle considering traffic signals. *in Proc. 9th IEEE Int. Conf. Power Electronics Drive Systems*, 733–738.

Monastyrsky, V. and Golownykh, I. (1993). Rapid computation of optimal control for vehicles. *Transportation Research Part B*, 27, 219–227.

Ozatay, E., Ozguner, U., Michelini, J., and Filev, D. (2014). Analytical solution to the minimum energy consumption based velocity profile optimization problem with variable road grade ? *19th World Congress*, 7541–754.

Perez, F., Moulin, P., and Mastro, A.D. (2008). Vehicle simulation on an engine test bed. *Proc. SIA Conference on Diesel Engines*.

Petit, N. and Sciarretta, A. (2011). Optimal drive of electric vehicles using an inversion-based trajectory generation approach. *18th IFAC World Congress*, 18, 14519–14526.

Sciarretta, A., Nunzio, G.D., and Ojeda, L.L. (2015). Optimal ecodriving control: Energy-efficient driving of road vehicles as an optimal control problem. *IEEE Control Systems Magazine*, 35.5, 71–90.

van Keulen, T., de Jager, B., Foster, D., and Steinbuch, M. (2010). Velocity trajectory optimization in hybrid electric trucks. *in Proc. American Control Conference*, 5074–5079.